

## A MODEL FOR THE CRACK INITIATION PROCESS IN COMPOSITE MATERIALS UNDER MULTIAXIAL FATIGUE LOADING

P. A. Carraro, M. Quaresimin \*

*Department of Management and Engineering, University of Padova, Stradella S. Nicola 3, Vicenza, Italy*

*\* marino.quaresimin@unipd.it*

**Keywords:** Multiaxial fatigue, Composites, Micromechanics

### **Abstract**

*In the present work a criterion for the matrix-controlled fatigue behavior of composite unidirectional laminae subjected to multiaxial loading is proposed. The criterion is based on experimental observations from previous works and from the literature concerning the damage modes occurring at the microscopic scale, bringing a lamina to fatigue failure. In particular two parameters have been identified as representative of the driving forces for the damage evolution, and they have to be used for design purposes depending on the multiaxiality condition. These parameters, i.e. the local maximum principal stress and first invariant of the stress tensor, are expressed in terms of local stresses in the matrix, calculated by means of finite element analyses of a fiber/matrix unit cell subjected to periodic boundary conditions. Applications of the proposed criterion to fatigue results from the literature show that only two scatter bands can be used to completely describe the multiaxial fatigue behavior of unidirectional laminae.*

### **1. Introduction**

Most of static and fatigue failure criteria for unidirectional (UD) composites are based on macromechanical quantities as the nominal stresses in the material coordinate system, which are often involved in a polynomial expression describing the failure condition. Tsai-Hill and Tsai-Wu are some classical examples for static behavior. An improvement is achieved by Puck's polynomial criterion [1], since it involves the macroscopic stresses lying on the fracture plane; however it is always a macroscopic and phenomenological criterion which does not account for the actual damage mechanisms at the microscopic scale. Concerning the fatigue behavior, some empirical criteria are available in the literature, providing sometimes not accurate predictions, as discussed in [2]. In addition, Kawai [3] extended the Tsai-Hill polynomial criterion to fatigue, combining it with a continuum damage model to obtain a power law for the S-N curves, but without taking into account the different damage mechanisms. Moreover, the fact of describing with one only equation the fatigue behavior for both fiber and matrix-dominated response seems not to have a physical meaning, in the authors' opinion. Before Kawai, Hashin and Rotem [4] proposed a polynomial criterion, separating the fiber and the matrix dominated behaviors, which have to be described with different expressions, to be used depending on which is the critical component in the composite lamina (fiber or matrix). In particular, for the matrix dominated behavior they proposed to involve in a polynomial expression only the transverse and in plane shear stresses, weighted by means of fatigue functions to be experimentally calibrated. Therefore, in spite of the merit of treating separately the fiber and matrix dominated behaviors, this criterion still considers the macroscopic nominal stresses, involved in a phenomenological expression. Concerning the non-fiber dominated behavior, some efforts in the direction of considering the local stresses (or micro-stresses) acting in the matrix have been published by Reifsnieder and Gao in 1991 [5]. They used the Mori-Tanaka theory in order to evaluate the

average transverse stress and in-plane shear stress in the matrix, involving them in a criterion similar to that of Hashin, using some fatigue function of empirical derivation. In spite of the use of the local average stresses, this is still a phenomenological criterion, and it requires a large experimental effort for the model calibration. In 1999 Plumtree and Cheng [6] developed a model based on the local stresses acting on the fracture plane, defined as the plane normal to the transverse direction. According to this definition of the fracture plane, the relevant stresses turned out to be the local transverse and in plane shear stresses only, calculated by means of Finite Element (FE) analyses of a fiber-matrix unit cell. In addition they took inspiration from the Smith-Watson-Topper (SWT) criterion for metals [7] to account for the presence of a non zero mean stress.

The aim of the present work is to define a physically based criterion, suitable to describe the non-fiber dominated fatigue behavior, in terms of crack initiation, of UD laminae subjected to multiaxial loading, characterized by the presence of the lamina stress components  $\sigma_1$ ,  $\sigma_2$  and  $\sigma_6$  (see figure 1 for the definition of stresses).

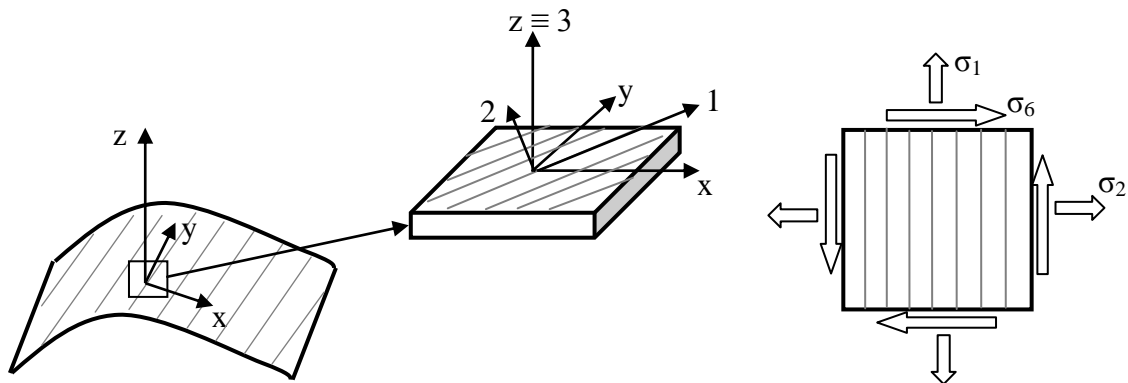


**Figure 1:** Global and local coordinate system, and stresses in the local coordinates system

The proposed model is based on the damage modes experimentally observed by the present authors [8] and from the literature, as will be better explained in the next section, and its application to a large bulk of experimental data reveals a good accuracy.

## 2. Mechanisms of fatigue failure

First of all, some preliminary considerations about the peculiarities of fatigue failure are needed. As is known from the literature, if an UD lamina is subjected to a cyclic loading condition leading to a matrix-dominated response, it fails without a visible progressive damage [8-10]. This means that a stable crack propagation is never observed and, conversely, when a macro-crack (visible crack) nucleates, it propagates unstably bringing the lamina to the complete fracture in just few cycles. Therefore, from many experimental evidences, it can be concluded that the matrix-dominated fatigue failure is controlled by the initiation phase, if the word “*initiation*” is referred to a macro-crack parallel to the fibers. However, at a microscopic level, a sort of degradation process has to take place during fatigue life, otherwise the decreasing trend of the fatigue S-N curves cannot be explained [11]. As a consequence, a driving force for the micro-damage progression leading to the final macro-crack onset has to be established, and it cannot be done regardless of the damage modes acting at the microscopic scale. In order to do that, the concept of the fracture plane is introduced in the following. As already mentioned, Puck’s criterion is based on the fact that the effective stresses to be considered as the cause of the static failure are the stresses lying on the fracture plane.

According to Puck, in the case of positive values of  $\sigma_2$  and  $\sigma_6$ , the fracture plane is always the plane whose normal is the transverse direction (2-axis), and therefore the effective stresses are the global stress components  $\sigma_2$  and  $\sigma_6$ . The importance of the fracture plane is emphasized also by Plumtree and Cheng [6], and also for them, in the case of an off-axis lamina, the stress components to be accounted for are  $\sigma_2$  and  $\sigma_6$  only, because they act on the plane normal to the 2-direction. The main merit of their criterion is that it considers the local stresses in the matrix, resulting from the concentrations due the presence of the fibers, instead of the global stresses.

It is important to underline that the fracture plane considered by Puck and by Plumtree-Cheng is actually a final separation plane, it can be named *macroscopic fracture plane*. The actual fracture plane, in which the matrix micro-cracking and the degradation process occurs, is not parallel to the fibers, and this is confirmed by experimental observations of the fracture surfaces that can be found in [8, 9]. In figure 2 the concept of the *microscopic fracture plane* is introduced, as the plane in which the micro-damage occurs by means of matrix micro-cracks.

### Macroscopic fracture plane

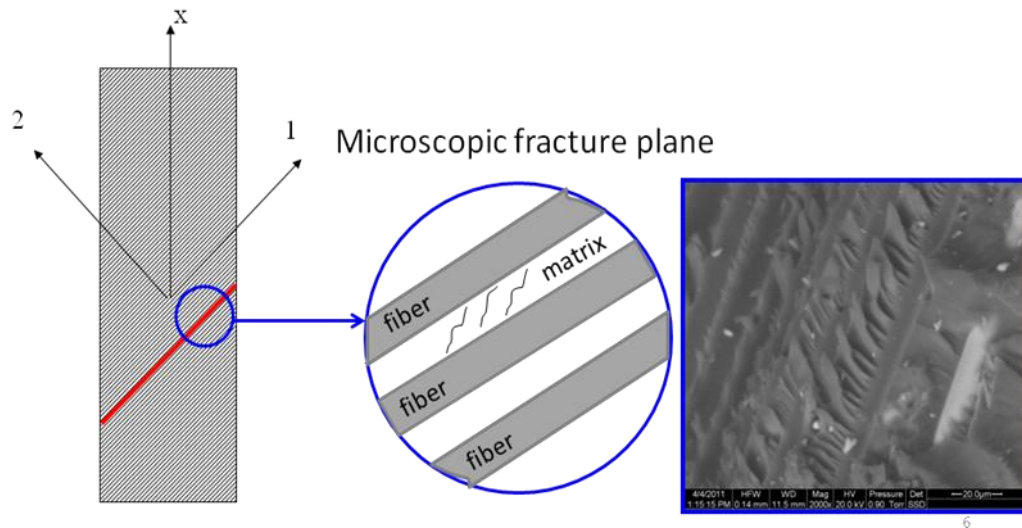


**Figure 2:** Concept of the microscopic fracture plane (picture from [8])

Therefore a criterion to assess the microscopic fracture plane is required, and in the present work it is considered as the plane perpendicular to the local maximum principal stress. As a consequence, the effective stress to be considered is the maximum principal stress (MPS) in the matrix, which has to be calculated by considering the local stress fields, i.e. the microstresses.

In addition, Asp et al.[12, 13] in 1996 proved that, since the local stress state at or close to the fiber-matrix interface is nearly hydrostatical, in the case of pure transverse tension, the matrix static failure is caused by the resin cavitation. Therefore a good criterion for predicting the composite failure in the case of pure transverse stress is based on reaching a critical value for the dilatational energy density expressed in equation (1):

$$U_v = \frac{1-2\nu}{6E} I_1^2 \quad (1)$$

where  $I_1$  is the first stress tensor invariant, which has to be calculated once again considering the local stress fields. In [13] good agreement was found between predictions based on this criterion and experimental results for the transverse static strength of a UD lamina.

Therefore it is reasonable to expect a change in the leading damage mode moving from a loading condition near the pure transverse stress to another one, characterized by the presence of an enough high shear stress component. According to this idea the following criterion for multiaxial fatigue is proposed: two different parameters, representative of two different driving forces, have to be used, according to the multiaxiality condition:

- the peak of the local value of  $I_1$ , for nearly pure transverse tension case;
- the peak of local maximum principal stress (MPS) for enough high shear stress component.

### 3. Calculation of the local stresses

As stated above, a driving force for the microscopic damage evolution has to be expressed in terms of local stresses (or micro-stresses) acting in the matrix and at the fiber-matrix interface. In the present work a regular square fibers array as in figure 3 is assumed for the sake of micro-stresses calculation. Of course it is not exactly representative of the real composite system, because of the non uniform actual fibers distribution, but it has been shown to provide good results in terms of stress concentrations, if compared to a random fiber array [14]. However, a reasonable simplification of the problem under analysis has to be accepted if a criterion of practical use and industrial appeal has to be formulated. Because of the geometrical symmetry only one quarter of a unit cell can be considered for the sake of calculation, as shown in figure 3.

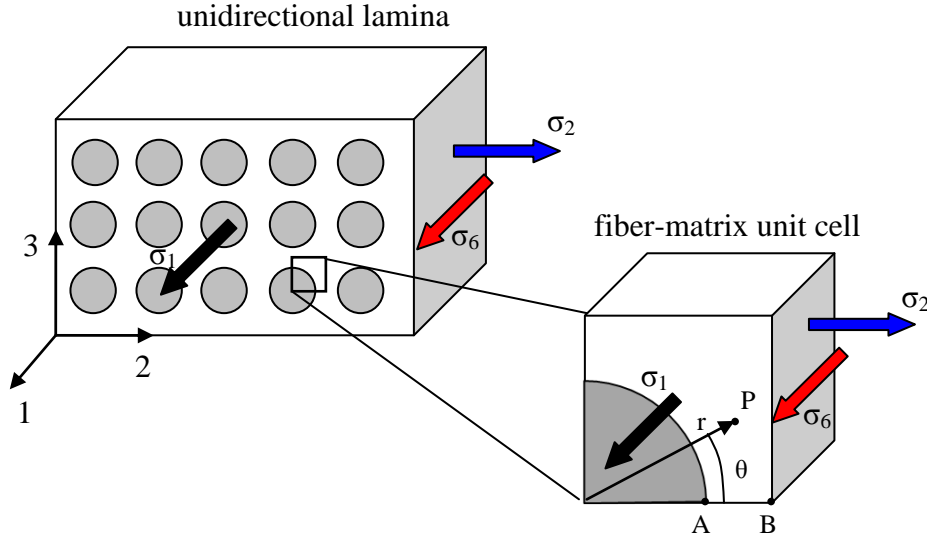


**Figure 3:** definition of the fiber-matrix unit cell for micromechanical analysis

The micro-stresses have been calculated by means of FE analyses of a fiber-matrix unit cell subjected to the average, or macroscopic stresses  $\sigma_1$ ,  $\sigma_2$  and  $\sigma_6$ . Periodic boundary conditions have been applied to the surfaces of the quarter of the unit cell as explained in [15]. In addition, also the residual stresses due to the cooling process after curing should be considered, and the thermal load has been applied as a uniform temperature jump  $\Delta T = T_c - T_r$ , where  $T_c$  is the curing temperature and  $T_r$  is the room temperature. Because the fatigue loads are lower than the static failure loads the matrix behavior is considered mostly linear, and therefore linear elastic analyses have been conducted with the software ANSYS 11<sup>®</sup> using 20 nodes solid elements.

At each point P of the unit cell the mechanical micro-stresses in polar coordinates  $(r, \theta, z)$  can be defined in terms of stress concentration factors  $k_{i,jl}$  relating the macro-stress  $\sigma_i$  with the local stress  $\sigma_{jl}$ , as in equation (2). Finally the thermal stresses are related to the temperature jump  $\Delta T$  by means of thermal concentration factors  $h_{jl}$ , as in equation (2).

$$\begin{Bmatrix} \sigma_{rr} \\ \sigma_{\theta\theta} \\ \sigma_{zz} \\ \sigma_{r\theta} \\ \sigma_{\theta z} \\ \sigma_{rz} \end{Bmatrix}^P = \begin{bmatrix} k_{1,rr} & k_{2,rr} & k_{6,rr} \\ k_{1,\theta\theta} & k_{2,\theta\theta} & k_{6,\theta\theta} \\ k_{1,zz} & k_{2,zz} & k_{6,zz} \\ k_{1,r\theta} & k_{2,r\theta} & k_{6,r\theta} \\ k_{1,\theta z} & k_{2,\theta z} & k_{6,\theta z} \\ k_{1,rz} & k_{2,rz} & k_{6,rz} \end{bmatrix}^P \begin{Bmatrix} \sigma_1 \\ \sigma_2 \\ \sigma_6 \end{Bmatrix} + \Delta T \begin{Bmatrix} h_{rr} \\ h_{\theta\theta} \\ h_{zz} \\ h_{r\theta} \\ h_{\theta z} \\ h_{rz} \end{Bmatrix}^P \quad (2)$$

The stress concentration factors are functions of the fiber volume fraction  $V_f$  and of the elastic properties of the fiber/matrix system. In the case of glass/epoxy composites, typical values for the

Young moduli  $E$  and Poisson's ratio  $\nu$  have been used in the subsequent analyses, and they are listed in table 1. It is worth mentioning that, being the glass fiber much stiffer than epoxy, the value of the stress concentration factors has a very low sensitivity to the Young modulus of the matrix. In fact, if it is varied from 2000 to 4000 MPa, the maximum variation of the stress concentration factors is around 3%, which can be considered negligible. The adopted Coefficients of Thermal Expansion (CTE) for the constituents are also listed in table 1.

	<b>E (MPa)</b>	<b><math>\nu</math></b>	<b>CTE (<math>^{\circ}\text{C}^{-1}</math>)</b>
<b>Glass</b>	70000	0.22	$7 \cdot 10^{-6}$
<b>Epoxy</b>	3200	0.37	$67.5 \cdot 10^{-6}$

**Table 1:** Typical glass/epoxy material properties used in the FE analyses

The peak values of the local MPS and  $I_1$  have been found to be always at the points A or B of figure 3 where, because of symmetry, some stress components vanish leading to the following expressions for MPS and  $I_1$ :

$$MPS = \frac{1}{2} \left[ \sigma_{rr} + \sigma_{zz} + \sqrt{\sigma_{rr}^2 + 4\sigma_{rz}^2 - 2\sigma_{rr}\sigma_{zz} + \sigma_{zz}^2} \right] \quad (3)$$

$$I_1 = \sigma_{rr} + \sigma_{\theta\theta} + \sigma_{zz} \quad (4)$$

where the stresses defined by equation (2) have to be substituted. According to the criterion proposed at the end of section 2, the MPS defined in equation (3) has to be used as fatigue parameter in order to present fatigue S-N data for different multiaxiality conditions, not nearly in pure transverse tension. Conversely, in such a condition the parameter  $I_1$  defined in equation (4) has to be used as representative of the driving force for damage evolution. In the following section the fatigue results from different works from the literature will be reanalyzed in terms of MPS and  $I_1$ .

## 4. Application to experimental data

### 4.1 Fatigue results on tubular specimens

In [8] the authors presented the experimental results on glass/epoxy pipes with the fibers oriented at  $90^{\circ}$  with respect to the axis of the tube, and subjected to combined tension-torsion cyclic loading, resulting in the stress components  $\sigma_2$  and  $\sigma_6$ . A parameter  $\lambda_{12} = \sigma_6/\sigma_2$  was defined [2] in order to describe the biaxiality of the stress state. In [8] fatigue curves were presented for  $\lambda_{12} = 0, 1$  and  $2$ , and in the present work some additional data are presented, for  $\lambda_{12} = 3$  and  $\infty$  (pure torsion). In figure 4a) the S-N curves are shown in terms of the maximum cyclic value of the transverse stress  $\sigma_{2,max}$ , revealing a very strong influence of the biaxiality ratio on the fatigue resistance. Obviously the data for the pure torsion case cannot be plotted in figure 4a), but they will be shown in the subsequent analysis.

In figure 4b) the fatigue data are plotted in terms of the maximum cyclic value of the local MPS, calculated by means of the micromechanical analysis described in section 3. It can be seen that the curves for  $\lambda_{12} \geq 1$  are reasonably well collapsed into a narrow scatter band, indicating that, in these conditions, the MPS is representative of the driving force for the damage evolution bringing the lamina to the fatigue failure. Conversely, lower values of MPS are found for the curve corresponding to  $\lambda_{12} = 0$  (pure transverse stress). This is not surprising, since the hydrostatic component of the stress tensor becomes dominant in such a condition, becoming the leading driving force for the damage progression, as reported in section 2. In fact, if all the curves are plotted in terms of the local value of  $I_1$ , the pure tension curve would be higher than the others. The figure is not shown for a matter of space, but the distribution of fatigue data is similar to that observed in figure 4a), being  $I_1$  dependent on  $\sigma_2$  and on the residual stresses only.

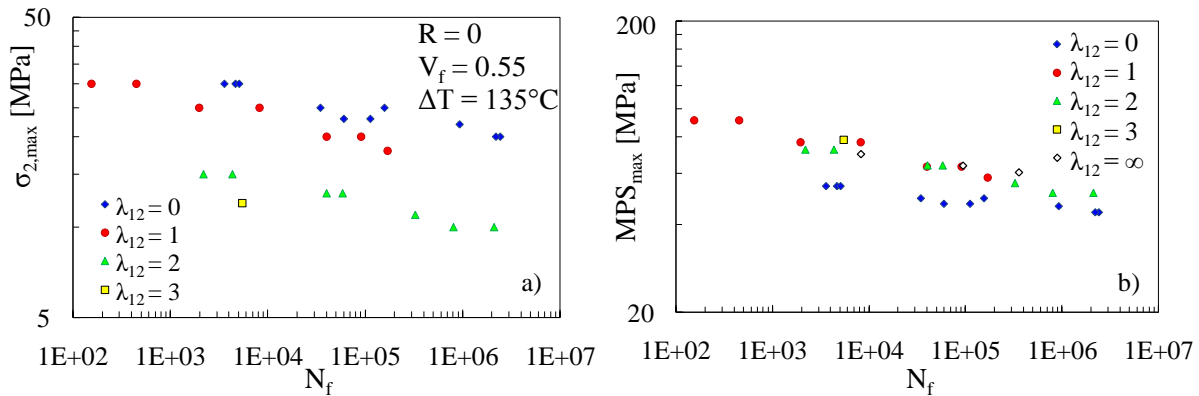


**Figure 4:** fatigue results for tubes: maximum a)cyclic transverse stress and b)MPS against the number of cycles to failure  $N_f$

#### 4.2 Fatigue results on flat specimens from Hashin and Rotem

In [4] Hashin and Rotem presented the results of fatigue tests on flat UD laminae subjected to off-axis loading, resulting in a multiaxial state with the presence of all the three in-plane stress components. In figure 5a) the results are shown in terms of the maximum cyclic value of the global applied stress in the loading direction  $\sigma_{x,max}$ . Different fatigue curves are related to different off-axis angles, if plotted in terms of the global stress, but they are well collapsed into a single scatter band if the local MPS is used to present fatigue data, as can be seen in figure 5b).

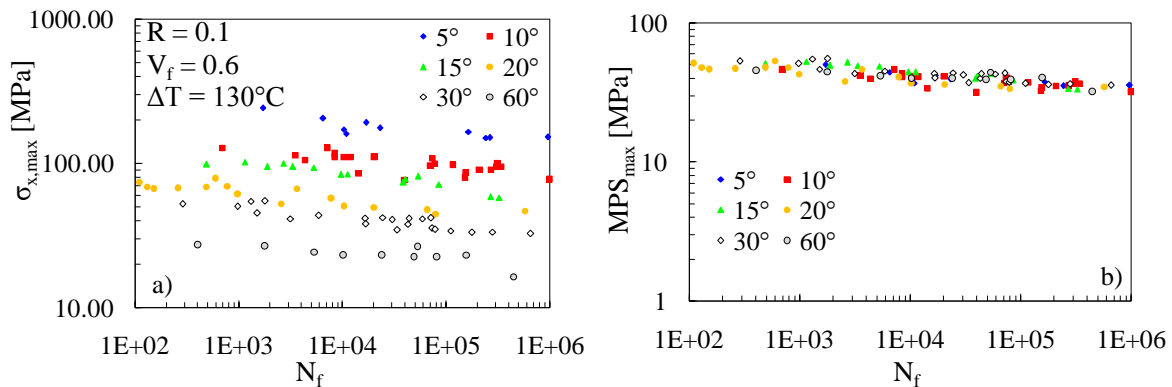


**Figure 5:** fatigue results on flat [4]: maximum a) cyclic global stress and b) MPS against the number of cycles to failure  $N_f$

In this case all the curves, for off-axis angles from 5 to 60 degrees, are well described by the MPS, which turns out to be once again a good parameter to represent the driving force for fatigue damage in loading conditions not nearly in pure transverse stress.

#### 4.3 Fatigue results on flat specimens from El Kadi and Ellyin

In [10] El-Kadi and Ellyin tested flat unidirectional specimens subjected to cyclic off-axis loading with three values of the stress ratio  $R$  (-1, 0, 0.5). It is important to say that the present criterion is valid for non negative stress ratios, because an eventual compressive part of the fatigue cycles could produce some damage modes different from those related to the tensile part, and therefore they should be described by different parameters. In the following only the results for  $R = 0$  are shown for a matter of space, but the case of  $R = 0.5$  leads to very similar conclusions. Figure 6 shows that different fatigue curves are obtained if the results are expressed in terms of the maximum applied stress in the loading direction.

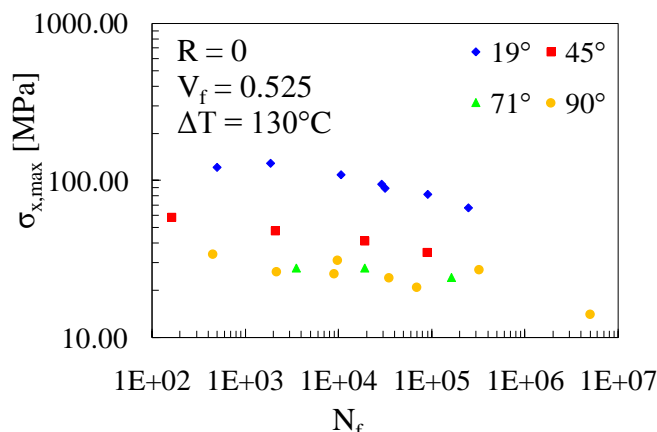


**Figure 6:** fatigue results on flat [10]: maximum cyclic global stress against the number of cycles to failure  $N_f$

In figure 7a) the results are reanalyzed in terms of the local MPS, where it can be noticed that the curves for off-axis angles of 19 and 45 degrees can be reasonably thought to be collapsed into a single scatter band, while the other curves clearly exhibit lower values of MPS. In fact these curve are related to loading conditions characterized by a highly hydrostatical local stress state and they exhibit higher values of the local  $I_1$ , as can be seen in figure 7b). The curve for 45° seems to be included in both the scatter bands, in terms of MPS and  $I_1$ , and this is probably because it is representative of a stress state close to the point of transition from one leading damage mode to the other.

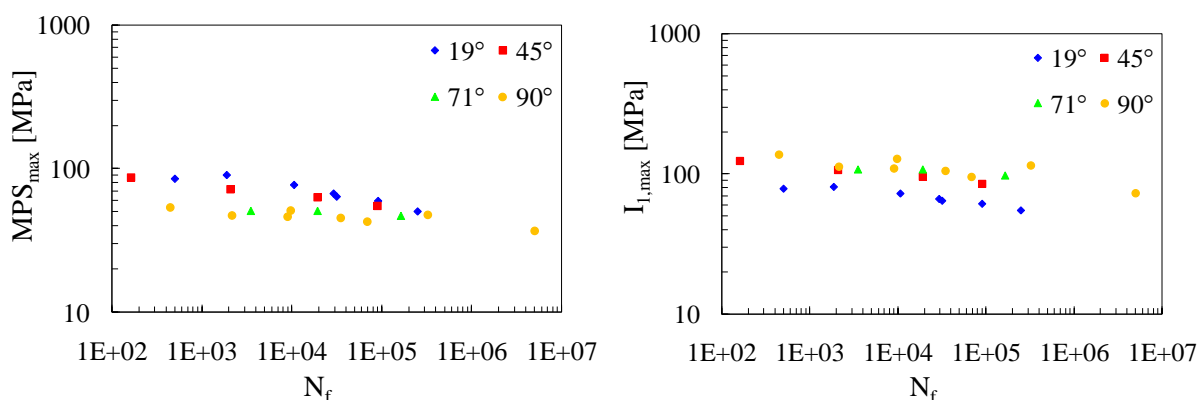


**Figure 7:** fatigue results on flat [10]: maximum a) MPS and b)  $I_1$  against the number of cycles to failure  $N_f$

## 5. Discussion and conclusions

A criterion for the description of the non-fiber dominated fatigue behavior of UD laminae has been proposed, suitable to deal with multiaxial conditions. The aim of the work was not to describe exactly the damage modes occurring at the microscopic scale, but to identify some parameters representative of the driving force for their evolution during fatigue life. According to experimental observations [8], the concept of the *microscopic fracture plane* has been introduced and it has been identified as the plane normal to the local Maximum Principal Stress (MPS) calculated by means of micromechanical tools. The MPS parameter has been found to collapse in one single scatter band the fatigue curves related to multiaxial loading conditions, not in nearly pure transverse stress. In fact it is proved [13] that in such conditions the local stress state in the matrix is highly hydrostatical, and it is reasonable to assume that this produces a change in the leading damage mode and therefore in the parameter to be used as representative of the driving force. In this work the local value of the first stress tensor invariant  $I_1$  has been shown to be a good parameter to collect fatigue data in the case of loading conditions with a low shear stress, compared to the transverse stress. Therefore only two scatter bands, and related master curves, can be used for multiaxial fatigue design of composite laminae, depending on the multiaxiality stress state. The condition corresponding to the transition between the two leading

damage modes is a property of the composite system and it can be easily calculated, but it will not be shown in the present work for a matter of space.

Finally, the present criterion is valid for positive stress ratios  $R$ , but even in this range it does not account for the effect of this parameter. In fact all the curves have been presented in section 4 in terms of maximum cyclic values of  $MPS$  and  $I_1$ , which are suitable to describe the fatigue curves for a fixed value of  $R$ . Further analyses are being conducted in order to understand the influence of the stress ratio and to include it in the criterion.

## References

- [1] Puck A., Shurmann H., Failure analysis of FRP laminates by means of physically based phenomenological models, *Composites Science and Technology*, **58**, pp. 1045-1067 (1998).
- [2] Quaresimin M., Susmel L., Talreja R., Fatigue behaviour and life assessment of composite laminates under multiaxial loadings. *International Journal of Fatigue*, **32**, pp. 2-16 (2010).
- [3] Kawai M., Yajima S., Hachinohe A., Takano Y., Off-axis fatigue behaviour of unidirectional carbon fiber-reinforced composites at room and high temperatures. *Journal of Composites Materials*, **35**, pp.545-576 (2001).
- [4] Hashin Z., Rotem A., A fatigue failure criterion for fibre-reinforced materials. *Journal of Composite Materials*, **7**, pp. 448-464 (1973).
- [5] Reifsnider K. L., Gao Z., A micromechanics model for composites under fatigue loading, *International journal of fatigue*, **13**, pp. 149-156 (1991).
- [6] Plumtree A., Cheng G. X., A fatigue damage parameter for off-axis unidirectional fiber reinforced composites, *International journal of fatigue*, **21**, pp. 849-856 (1999).
- [7] Smith K.N., Watson P., Topper T.H., A stress strain function for the fatigue of metals. *Journal of Materials*, **5**, pp. 767-778 (1970).
- [8] Carraro P. A., Quaresimin M., Fatigue damage evolution in  $[0_F/90_{U,3}/0_F]$  composite tubes under multiaxial loading in "Proceeding of 18th International Conference on Composite Materials", Jeju Island, Korea, August 21-26 2011.
- [9] Awerbuch J., Hahn H. T., Off-axis fatigue of graphite/epoxy composite. *Fatigue of Fibrous Composite Materials*, ASTM STP 723, American Society for Testing and Materials, pp.243-273 (1981).
- [10] El-Kadi H., Ellyin F., Effect of stress ratio on the fatigue of unidirectional fiberglass-epoxy composite laminae. *Composites*, **25**, pp. 917-923 (1994).
- [11] Talreja R., Fatigue of Composite Materials: Damage Mechanisms and Fatigue-Life Diagrams, *Proceedings of the Royal Society of London. Series A, Mathematical and Physical Sciences*, **378**, pp. 461-475 (1981).
- [12] Asp L. E., Berglund L. A., Talreja R., A criterion for crack initiation in glassy polymers subjected to a composite-like stress state, *Composites Science and Technology*, **56**, pp. 1291-1301 (1996).
- [13] Asp L. E., Berglund L. A., Talreja R., Prediction of matrix initiated transverse failure in polymer composites, *Composites Science and Technology*, **56**, pp. 1089-1097 (1996).
- [14] Huang Y., Jin K. K., Ha S. K., Effects of Fiber Arrangement on Mechanical Behavior of Unidirectional Composites, *Journal of Composite Materials*, **42**, 1851-1871 (2008).
- [15] Zhang Y., Xia Z., Micromechanical Analysis of Interphase Damage for Fiber Reinforced Composite Laminates, *CMC*, **2**, pp.213-226 (2005).